Applied Energy 112 (2013) 533–538

Contents lists available at SciVerse ScienceDirect

Applied Energy

journal homepage: www.elsevier.com/locate/apenergy

Production of cyclohexane from lignin degradation compounds over $Ni/ZrO_2–SiO_2$ catalysts

Xinghua Zhang [a,b], Tiejun Wang [a,*], Longlong Ma [a,*], Qi Zhang [a], Xiaoming Huang [a,b], Yuxiao Yu [a,b]

[a] *Key Laboratory of Renewable Energy and Gas Hydrate, Guangzhou Institute of Energy Conversion, Chinese Academy of Sciences, Guangzhou 510640, PR China*
[b] *Graduate School of Chinese Academy of Science, Beijing 100049, PR China*

HIGHLIGHTS

- $ZrO_2–SiO_2$ mixed oxides as catalyst supports.
- $ZrO_2–SiO_2$ mixed oxides possess amphoteric character and excellent textural properties.
- Phenol and guaiacol were completely converted over $Ni/ZrO_2–SiO_2$ catalyst.
- The selectivity for the desired product cyclohexane was in excess of 90%.

ARTICLE INFO

Article history:
Received 18 September 2012
Received in revised form 8 March 2013
Accepted 26 April 2013
Available online 20 May 2013

Keywords:
Lignin
Phenolic compounds
$Ni/ZrO_2–SiO_2$
Cyclohexane
Hydrodeoxygenation (HDO)

ABSTRACT

The main products of lignin degradation are phenolic compounds. It is meaningful to study the processes by which cyclohexane is produced from phenolic compounds via hydrodeoxygenation (HDO), because it could be used as fuel additives, chemical feedstock and solvent. In this work, support material $ZrO_2–SiO_2$ mixed oxides with different Si/Zr ratio were synthesized, and a series of $Ni/SiO_2–ZrO_2$ catalysts with different Ni loading were prepared by impregnation method. The exploration of HDO process was carried out using phenol and guaiacol as model compounds. Effects of Si/Zr ratio, Ni loading and reaction temperature on conversion of phenol and guaiacol as well as distribution of HDO products were systematically investigated. The results showed that almost all of phenol and guaiacol could be effectively converted into O-free products. And the selectivity of cyclohexane was in excess of 90%.

© 2013 Elsevier Ltd. All rights reserved.

1. Introduction

Lignocellulosic biomass contains three kinds of components (cellulose, hemicelluloses and lignin) [1]. Generally, the components of cellulose and hemicelluloses could be converted into ethanol fuels by hydrolysis and fermentation processes [2–5]. However, the lignin is not amenable to such a conversion. Thus, the expected growth of the production capacity of second-generation bio-fuels from biomass by fermentation processes will lead to a vast source of lignin [6]. Besides, large amounts of lignin and lignin-containing residues originate from the pulp and paper industry every year [7]. Phenolic compounds such as phenol and guaiacol can be produced easily though lignin pyrolysis, or lignin catalytic liquefaction [8,9]. Especially, phenolic compounds can be obtained directly from bio-oil derived from fast pyrolysis of biomass [6,10]. These phenolic compounds cannot be used as engine fuels directly due to their high oxygen content, poor chemical stability, corrosivity and immiscibility with hydrocarbon fuels [11]. It is also difficult to purify these phenolic compounds for production of fine chemical due to the complex composition. Therefore, for better uses of phenolic compounds derived from lignin, process of hydrodeoxygenation (HDO) is needed.

In the research field of HDO for oxygenated compounds, conventional hydrodesulfurization (HDS) catalysts – sulfided CoMo and NiMo supported on Al_2O_3 were explored originally by the majority of researchers [12–14]. The Co promoting effect on MoS_2 phase in the guaiacol hydrodeoxygenation reaction was reported in details [15]. However, the sulfur-containing compounds, such as mercaptan, were observed in liquid products [15]. These sulfur-containing compounds may give rise in contamination of produced hydrocarbons, although it is minor. In addition, regarding alumina support, there are two disadvantages: first, alumina support induced the production of heavier products which certainly contributed to catalyst deactivation [16]; second, alumina is known to be metastable in the presence of water, and will partially transform into boehmite under hydrothermal conditions [17]. ZrO_2 was considered as an appropriate support for HDO cat-

---

* Corresponding authors. Tel.: +86 20 8705 7673; fax: +86 20 8705 7789.
E-mail addresses: wangtj@ms.giec.ac.cn (T. Wang), mall@ms.giec.ac.cn (L. Ma).

0306-2619/$ - see front matter © 2013 Elsevier Ltd. All rights reserved.
http://dx.doi.org/10.1016/j.apenergy.2013.04.077

alysts because the ZrO_2 support appears to favor activation of O-compounds in the support surface [16].Nevertheless, the surface area of ZrO_2 is very small. This is unfavorable for the improvement of catalytic performance. The addition of SiO_2 into ZrO_2 may overcome this disadvantage. In addition, the interaction of ZrO_2 and SiO_2 exhibited some unique physical and chemical properties.

Thus, in this work, the binary ZrO_2–SiO_2 mixed oxide was synthesized as a support for the hydrodeoxygenation catalyst. The non-sulfided and cheap catalysts (using metal Ni as active component) were prepared by wetness precipitation method. And these catalysts were applied to catalytic HDO reaction for cycloehxane production from phenolic compounds. It is desirable to use phenol and guaiacol as model compounds for lignin-derived phenolic compounds for initial screening, while leaving the investigation of other phenolic compounds and optimization of catalysts as the subject of further research.

2. Materials and methods

2.1. Catalyst preparation

A series of ZrO_2–SiO_2 supports with varying molar ratio of Si/Zr were prepared as the following method. Appropriate amounts of $Na_2SiO_3 \cdot 9H_2O$ and $ZrOCl_2 \cdot 8H_2O$ were dissolved in distilled water respectively. With the continuously stirring, the solution of ammonium nitrate was dropped gradually into the solution of Na_2SiO_3 until the pH of the solution reached an approximate value of 8.0, by which the $Si(OH)_4$ precipitate was prepared. According to the similar procedure, the solution of ammonia was dropped into the solution of $ZrOCl_2$ until the pH of the solution reached an approximate value of 8.0, by which the $Zr(OH)_4$ precipitate was prepared. These two kinds of precipitates were mixed and whisked. The mixed precipitate was aging for 12 h at the temperature of 75 °C. Subsequently, the precipitate was filtered and washed with distilled water to completely remove chloride ions. The solid obtained was dried overnight at 120 °C and then calcined at 500 °C for 5 h, by which the porous mixed oxide was prepared. These samples are denoted as SZ-*n* (*n* is the Si/Zr molar ratio).

The Ni-based catalysts were prepared by wetness precipitation method. The Ni loading were 5, 10, 15, 20 wt.% respectively. The catalysts were designated as *x*Ni/SZ-*n* (*x* is the Ni loadings). All the catalysts were crushed and sieved to 120–200 BSS mesh, and reduced at 500 °C before use.

2.2. Catalyst testing

All the HDO catalytic reactions of phenolic compounds were carried out in a 500 ml stainless autoclave equipped with an electromagnetic driven stirrer. For each run, 1.5 g catalyst, 10.0 g of reactants and 100.0 g of solvent dodecane were loaded in the autoclave. The reactor was pressurized with H_2 to 5.0 MPa in order to keep the mole ratio of H_2 to reactants at about 10:1. The autoclave was heated to a desired reaction temperature, while the reagents were vigorously stirred at a rate of 800 rpm.

2.3. Characterization and analysis

The BET surface area, External Surface Area, Average Pore Diameter and pore volume of catalysts were determined by N_2 isothermal (77 K) adsorption using a QUADRASORB SI analyzer equipped with QuadraWin software system.

The supports and catalysts were also characterized By X-ray diffraction (XRD) (XPert Pro MPD with Cu Kα (λ = 0.154) radiation, Philip).

Ni dispersion degrees for the catalysts of Ni/SZ with various Ni loadings were determined by H_2 chemisorption using a Quantachrome-ASIQACIV200-2 automated gas sorption analyzer.

H_2-TPR (H_2 temperature-programmed reduction) studies were carried out in a quartz tube reactor. 50 mg of catalyst was pretreated in a flow of helium (30 ml/min) at 400 °C for 1 h to remove undesirable physisorbed species, and after cooling to room temperature, the sample was heated in a flow of $5\%H_2 + 95\%N_2$ (30 ml/min) from 100 to 650 °C at a heating rate of 10 °C/min. Hydrogen consumption was monitored by the change of thermal conductivity of the effluent gas stream, and calculated by external standard method using H_2-TPR of CuO as standard. The reduced NiO was calculated according to the hydrogen consumption, and the reduced degree was obtained by the reduced NiO divided by the Ni loadings.

NH_3-TPD and CO_2-TPD (NH_3 and CO_2 temperature-programmed desorption) studies were carried out in a quartz tube reactor equipped with TCD (thermal conductivity detector). Similar procedure was reported in a literature [18]. The amount of NH_3 desorbed per gram of sample was calculated by external standard method based on the injection of known volumes of the He–NH_3 mixture under the same conditions. Similarly, the amount of CO_2 desorbed per gram of sample was also determined.

The components of liquid products was confirmed by GC–MS (gas chromatography–mass spectrometry, SHIMADZU GC–MS-QP5050A) equipped with a DB-1 pack column (30 m × 0.2 mm × 0.2 μm quartz capillary column). Quantitative analysis of liquid products were performed by GC (SHIMADZU GC2010 with a flame ionization detector (FID) and a DB-5 column, 30 m × 0.25 mm × 0.1 μm, N_2 as carrier gas) with benzyl alcohol as the internal standard.

The conversions of reactant and the product distributions were calculated according to the following formulas:

$$X = \frac{m(\text{Reactant})_{in} - m(\text{Reactant})_{out}}{m(\text{Reactant})_{in}} \times 100\% \qquad (1)$$

$$P_i = \frac{m(\text{products})_i}{\sum_{i=j}^{n} m(\text{product})_i} \times 100\% \qquad (2)$$

3. Results and discussion

3.1. Characterization of supports and catalysts

The XRD patterns of support material ZrO_2 and SZ-3 are shown in Fig. 1. The XRD results show that pure ZrO_2 has two coexisting

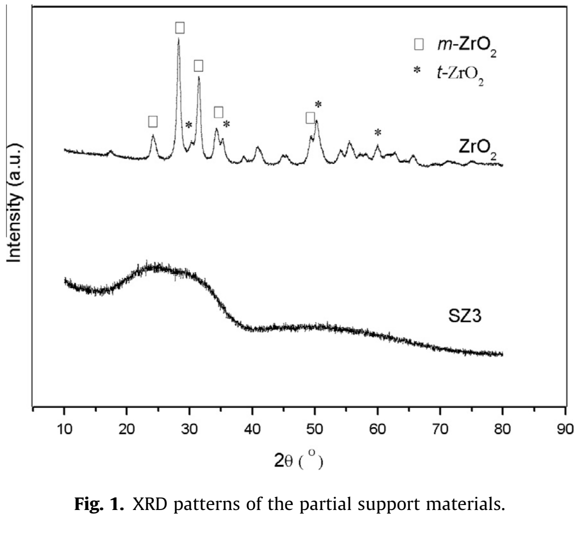

Fig. 1. XRD patterns of the partial support materials.

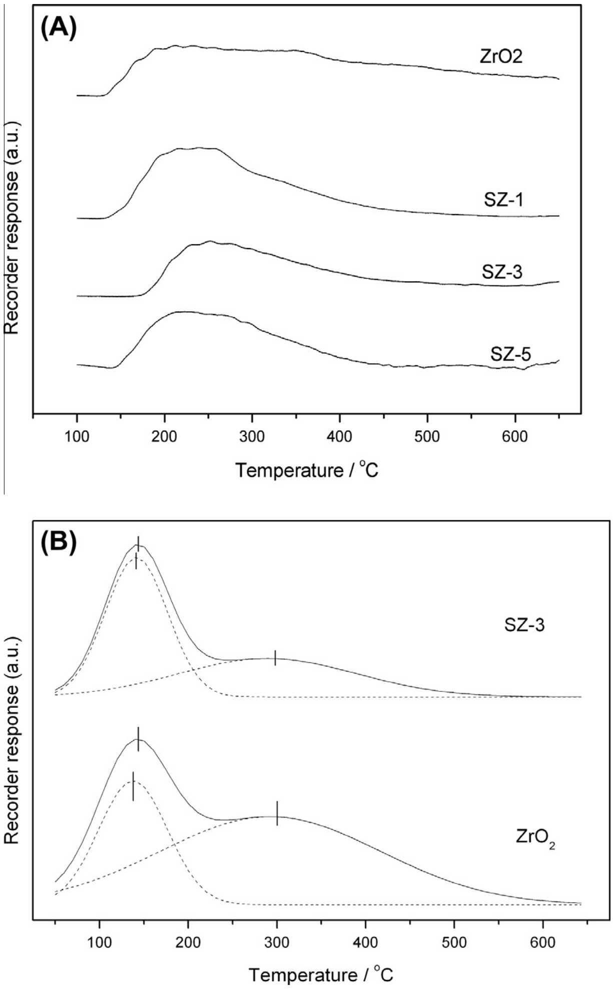

Fig. 2. NH_3-TPD and CO_2-TPD profiles of the different support samples. (A) NH_3-TPD profiles; (B) CO_2-TPD profiles.

structurally stable phase, namely monoclinic and tetragonal phases (m-ZrO_2 and t-ZrO_2). The 2θ for 24.1°, 28.2°, 31.4°, and 34.1° are assigned to the m-ZrO_2, and the peaks centered at 35.2°, 50.2°, 60.3° are assigned to the t-ZrO_2. It is reported that the t-ZrO_2 could transform into m-ZrO_2 with increasing of calcination temperature [19]. The SZ-3 mixed oxide, being an amorphous material, show no distinct XRD peaks apart from a very broad weak feature between 18°and 37°. All of the SZ samples with different Si/Zr ratio also show the similar broad feature (herein is not shown).

It is well know that ZrO_2 is an amphoteric oxide. To test the effect of SiO_2 on amphoteric character of ZrO_2, the NH_3-TPD and CO_2-TPD experiments for support materials were carried out and the results were presented in Fig. 2. Based on the desorption curves of NH_3, the amount and strength of acidic sites were determined and the results were listed in Table 1. It could be found that the addition of SiO_2 can increase the overall acid amounts of zirconia. Moreover, compared with ZrO_2, the highest peaks of mixed SZ composite moved to higher temperature, suggesting that the SZ composite exhibits higher acid strength since that the peak at higher temperature originates from the desorption of NH_3 from stronger acidic sites[20]. Among these SZ composites, the acid strength of SZ-3 is the strongest.

The CO_2-TPD analysis of ZrO_2 and SZ-3 (Fig. 2B and Table 1) show two desorption peaks of CO_2 centered at about 140 and 300 °C. Generally, different peaks in the CO_2-TPD profiles can differ base strength from a kind of basic site from another by their positions, and the amount of basic sites can be estimated by the amount of desorption CO_2. From the desorption peak of CO_2 centered at 140 °C, it could be found that the amount of weak basic sites for SZ-3 is closed to ZrO_2, suggesting that the addition of SiO_2 does not greatly affect on the weak basic sites of ZrO_2. However, compared with ZrO_2, the amount of strong basic sites for SZ-3 decreased obviously.

Textural properties of the catalysts are shown in Table 2 and Fig. 3. The BET surface area and total pore volume of catalysts supported on ZrO_2 are very small, and the pore distribution patterns show a small peak at about 2 nm besides the wide peak from 30 to 60 nm. For the catalysts supported on SZ mixed oxides, an apparent increase in BET surface area and total pore volume is observed. From Fig. 3, an apparent peak centered at about 10 nm is found for the catalysts supported on SZ mixed oxides, indicating that the mesopore is the main pore structures. The textural differences suggested that the addition of SiO_2 leads to conspicuous changes in physical properties for catalysts.

From Table 2, it can also be found that the BET surface area, total porous volume, and average pore size decreased with increasing of Ni loadings, which can be attributed to the increase of Ni load-

Table 1
The amounts of desorbed NH_3 and CO_2 for different support materials.

NH_3-TPD			CO_2-TPD		
Sample	Peak position (°C)	Amount of desorbed NH_3 (mmol g^{-1})	Sample	Peak position (°C)	Amount of desorbed CO_2 (mmol g^{-1})
ZrO_2	210	0.53	ZrO_2	142	0.17
SZ-1	235	1.28		300	0.31
SZ-3	258	0.95	SZ-3	142	0.18
SZ-5	215	1.01		300	0.11

Table 2
Textural and structure properties of the Ni-based catalysts.

Catalysts	S_{BET} (m^2/g)	V_{total} (m^3/g)	D_p (nm)	Size of NiO crystal[a] (nm)	Reduced degree (%)	Ni dispersion[b] (%)
$10Ni/ZrO_2$	6.21	0.064	41.4	50.7	79.3	–
5Ni/SZ-3	244.4	0.78	12.7	25.7	88.7	12.61
10Ni/SZ-1	221.6	0.69	12.5	29.9	72.5	–
10Ni/SZ-3	228.8	0.69	12.1	29.3	73.5	9.18
10Ni/SZ-5	230.0	0.71	12.3	29.0	76.1	–
15Ni/SZ-3	205.9	0.68	13.2	29.4	67.4	4.05
20Ni/SZ-3	192.14	0.56	11.6	32.2	66.8	2.67

[a] The catalysts were in oxide state, and the average sizes of NiO were calculated by Scherrer equation.
[b] Determined by H_2 chemisorption.

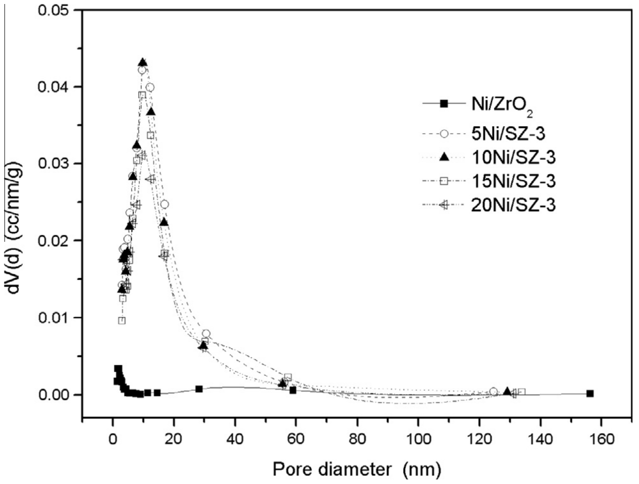

Fig. 3. Pore size distributions of Ni-based catalysts.

ings giving rise to aggregation of Ni particles, and the newly formed Ni clusters might block some meso-pores. This is accord with the Ni dispersion degree of catalysts, which decreased with increasing of Ni loadings. In addition, the size of NiO crystal calculated by Scherrer equation was also affected by the Ni loadings.

H_2-TPR experiments for Ni/SZ-3 catalysts with different Ni loadings were carried out and the results were presented in Fig. 4. A reduction peak centered at about 400 °C is common for all the profiles owing to the reduction of NiO weakly interacted with support material. The profile of 5Ni/SZ-3 catalyst shows a two-stage reduction behavior. A small reduction peak centered at 570 °C was observed only for the 5Ni/SZ-3 owing to the strong interaction with support material. It could be found that the NiO was well dispersed on the support while the Ni loadings was 5 wt.% from Table 2, this might be the reason that the NiO could strongly interacted with the support. The reduced degree of Ni-based catalysts decreased with increasing of Ni loadings, which might be resulted from the inefficiency of the H_2 reduction due to aggregation of partial Ni particles. Moreover, the reduction peak broadened gradually with the increasing of Ni loadings due to the mass transport limitation, which afforded additional supports for the inefficiency of the H_2 reduction with increased Ni loadings from another point of view.

3.2. HDO reaction of phenol

Conversions for HDO reaction of phenol over different catalysts at 300 °C are listed in Table 3. The experimental results indicate that the activities of catalysts supported on mixed oxides are obviously higher than those of catalysts supported on ZrO_2 alone under the same reaction conditions. There are two possible reasons account for this result. Firstly, the BET surface area of catalysts supported on ZrO_2 was obviously smaller than that of SZ mixed oxides. Larger BET surface facilitates the diffusion of reactants and reaction products, hence more complete reactions and higher conversion. Secondly, the NH_3-TPD experiments of different supports discussed above shown that the acid strength and overall acid amounts of SZ were superior to those of ZrO_2. It was reported that acid sites was related to hydrogenation, isomerization and cracking functionality [21]. Furthermore, the acid sites of supports can catalyze the dehydration reaction during the hydrodeoxygenation reaction, which could co-work well together with metal-catalyzed hydrogenation, and promoting oxygenates HDO reaction [18]. Moreover, the catalytic activity of the catalyst supported on SZ-3 was superior to those of the catalysts supported on SZ-1 and SZ-5. This further confirmed that the increased acid strength could favor the HDO reaction of phenol.

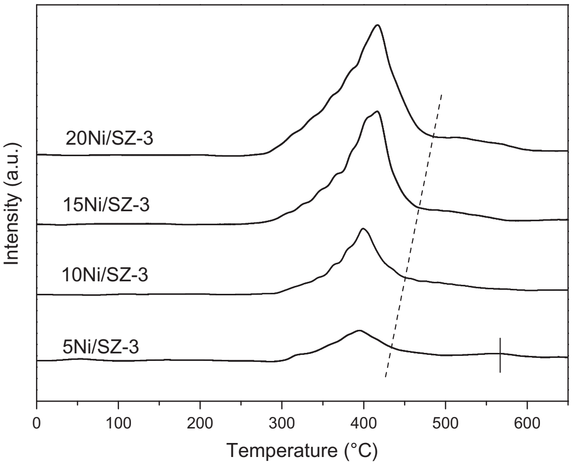

Fig. 4. H_2-TPR profiles of the Ni-based catalysts.

Table 3
Conversion of phenol over different catalysts (300 °C, 5.0 MPa).

Entry	Catalysts	Conversion (%)
1	$10Ni/ZrO_2$	36.7
2	10Ni/SZ-1	92.2
3	10Ni/SZ-3	100
4	10Ni/SZ-5	83.7
5	5Ni/SZ-3	85.1
6	15Ni/SZ-3	91.7
7	20Ni/SZ-3	77.5

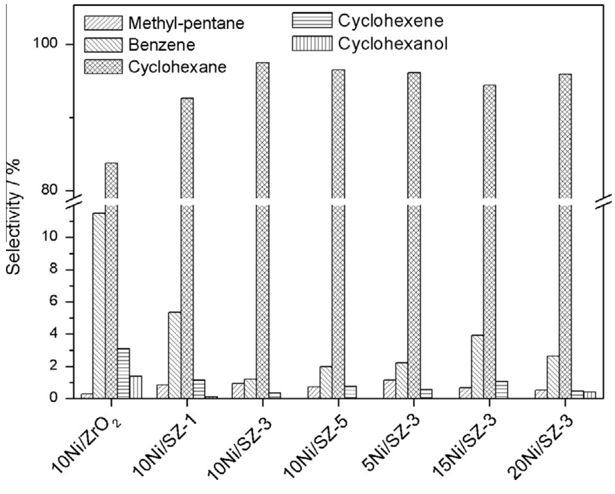

Fig. 5. Distribution of main products over different catalysts.

It can also be seen from Table 3 that the conversions of phenol were related to the loadings of Ni. A maximum was observed over 10Ni/SZ-3 catalyst. Beyond this loading amount, a decrease of conversion took place, especially for 20Ni/SZ-3 catalyst, which can be attributed to the decrease of Ni dispersion of catalysts, thereby leading to the decline of catalyst activity. However, the phenol conversion for the 5Ni/SZ-3 catalyst was lower, though its Ni dispersion was relative high. It could be speculated that the quantity of active Ni particles is small due to the lower Ni loadings. Thus, the Ni-catalyzed hydrogenation and solid acid-catalyzed dehydration could not co-work well, and leading to the decline of phenol conversion.

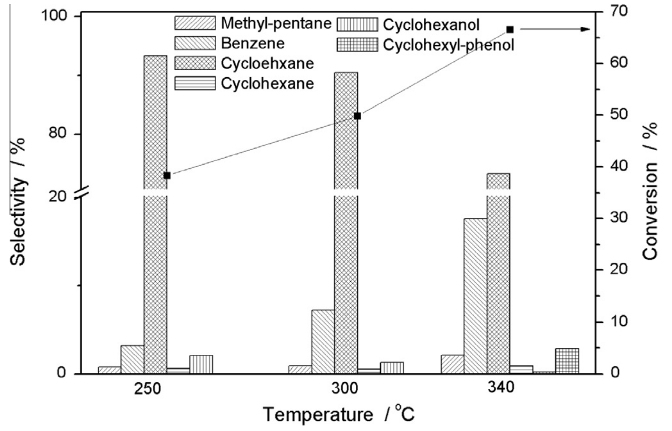

Fig. 6. Product distributions and phenol conversions as the temperature function over 10Ni/SZ-3 catalyst.

Fig. 5 shows the distributions of product derived from catalytic HDO of phenol over different catalysts. It can be seen that these catalysts exhibited excellent selectivity for the desired cyclohexane. And the selectivity of cyclohexane was in excess of 90% except for 10Ni/ZrO_2 catalyst. From Fig. 5, it can also be found that the Ni loadings of catalysts and Si/Zr ratios of supports have some effects on the selectivity for byproduct, such as methyl-cyclohexane, benzene and cyclohexanol. For example, the content of benzene was about 11% in the products obtained from phenol HDO over 10Ni/ZrO_2, while there was only a very small part in products obtained from phenol HDO over other catalysts. Cyclohexanol was only observed in HDO products over 10Ni/ZrO_2, 10Ni/SZ-1 and 20Ni/SZ-3, and was not detected in the products over 10Ni/SZ-3, 10Ni/SZ-5, 5Ni/SZ-3 and 15Ni/SZ-3.

In Fig. 6, the phenol conversion and product distributions are presented as the function of the reaction temperature over 10Ni/SZ-3 catalyst. In order to explore the reaction pathway of phenol HDO, the results was obtained under far from equilibrium through shorten reaction time. In the temperature range of 250–340 °C, phenol conversion increased with the increasing of temperature. This suggests that higher temperature could promote the phenol HDO reaction.

Table 4
Conversion of guaiacol and selectivity for main products.

Catalysts	Ni/SZ-3		
Temperature (°C)	250	300	340
Conversion (%)	67.3	100	100
Product distributions (%)			
Benzene	1.1	0.2	6.3
Cyclohexane	93.3	96.8	60.2
Cyclohexene	1.7	1.6	–
Methyl-cyclohexane	0.9	1.1	1.8
Toluene	0.6	0.3	0.5
Anisole	0.7	–	0.9
Phenol	1.7	–	10.3
Catechol	–	–	18.4
Phenyl-anisole	–	–	1.6

From Fig. 6, it could also be found that the reaction temperature has a pronounced effect on product distributions. The selectivity for cyclohexane decreases with increasing of reaction temperature. The selectivity for cyclohexanol decreases with increasing of reaction temperature, which could be attributed to the dehydration of cyclohexanol at higher temperature. On the contrary, the selectivity for benzene increases with increasing of reaction temperature. It could be concluded clearly that hydrogenolysis reaction of phenol to benzene is more favorable at a higher temperature. This conclusion is in a good agreement with the studies by Gandarias et al. [22] and Yang et al. [11]. Based on the experimental results, a tentative reaction pathway of phenol HDO was proposed (Fig. 7), and in which two main routes were presented: (1) direct elimination of hydroxyl group by hydrogenolysis of phenol; and (2) indirect elimination of hydroxyl group by thermal dehydration of a saturated cyclic alcohol formed by hydrogen addition to the aromatic ring.

As discussed above, HDO conversion increased with increased reaction temperature. However, the selectivity for benzene also increased due to a higher contribution of the hydrogenolysis route at a higher reaction temperature. Thus, the reaction temperature

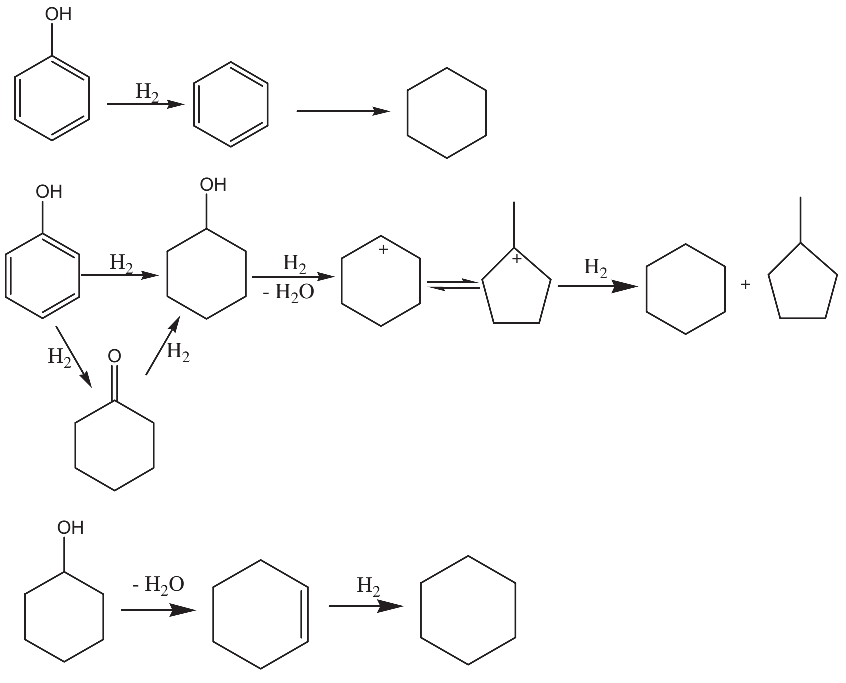

Fig. 7. Possible reaction pathways for the HDO of phenol.

should be treated carefully, in order to obtain an optimum balance between phenol HDO conversion and cyclohexane selectivity.

3.3. HDO reaction of guaiacol

Guaiacol was also chosen as model compounds for lignin-derived oxygenated compounds since its structure is similar to the monomer of lignin deconstruction containing three types of C–O bonds for C_{AR}–OH, C_{AR}–OCH_3 and $C_{AR}O$–CH_3. The HDO reaction of guaiacol was carried out over the optimal 10Ni/SZ-3 catalyst at different temperature, and the results were presented in Table 4. From Table 4, it could be seen that guaiacol shown a complete conversion at the temperature of 300 °C. The selectivity for desired product cyclohexane was 96.8%. This is a comparable result with the data obtained from phenol HDO. However, guaiacol HDO reaction is sensitive to temperature due to trend of polymerize at higher temperature [23]. From Table 4, it could be known that the selectivity for cyclohexane was only 60.2% at the temperature of 340 °C, although the conversion of guaiacol was 100%. Obviously, partial of guaiacol were converted into oxygenate compounds anisole, phenol and catechol. And phenyl-anisole was also observed in the HDO products, implying that the intermolecular polymerization occurred during the HDO processing of guaiacol at higher temperature. Moreover, a small party of guaiacol would be converted into polymers, which were the precursors of coke deposited on the surface of catalyst and resulted in deactivation.

4. Conclusions

In this work, a series of ZrO_2–SiO_2 mixed oxides (SZs) with different Si/Zr ratio were synthesized as a support materials. And the Ni/SZ catalysts prepared by wetness precipitation method exhibited excellent textural and structure properties compared with Ni/ZrO_2 catalyst. These catalysts were evaluated through HDO reaction using phenol and guaiacol as model compounds. The results showed that the conversion of phenol and guaiacol were almost 100%, and the selectivity for desired product cyclohexane was in excess of 90% under the optimum conditions, suggesting Ni/SZ catalysts possess excellent catalytic properties for production of cyclohexane from lignin-derived oxygenated compounds via HDO process.

Acknowledgements

This work was supported by grants from the National Natural Science Foundation of China (Project No. 51106167), National science and technology Project founded by MOST of China (Project No. 2012AA101808), and the International S&T Cooperation Program of China (Project No. 246772, 2012DFA61080).

References

[1] Chen WH, Cheng WY, Lu KM, Huang YP. An evaluation on improvement of pulverized biomass property for solid fuel through torrefaction. Appl Energy 2011;88:3636–44.

[2] Zheng Y, Yu C, Cheng YS, Lee C, Simmons CW, Dooley TM, et al. Integrating sugar beet pulp storage, hydrolysis and fermentation for fuel ethanol production. Appl Energy 2012;93:168–75.

[3] Tian S, Zhu J, Yang X. Evaluation of an adapted inhibitor-tolerant yeast strain for ethanol production from combined hydrolysate of softwood. Appl Energy 2011;88:1792–6.

[4] Mussatto SI, Machado EMS, Cameiro LM, Teixeira JA. Sugars metabolism ethanol production by different yeast strains from coffee industry wastes hydrolysates. Appl Energy 2012;92:763–8.

[5] Ilic DD, Dotzauer E, Trygg L. District heating and ethanol production through polygeneration in Stockholm. Appl Energy 2012;91:214–21.

[6] Zakzeski J, Bruijnincx PCA, Jongerius AL, Weckhuysen BM. The catalytic valorization of lignin for the production of renewable chemicals. Chem Rev 2010;110:3552–92.

[7] Laurijssen J, Faaij A, Worrell E. Energy conversion strategies in the European paper industry – a case study in three countries. Appl Energy 2012;98:102–13.

[8] Lou R, Wu SB. Products properties from fast pyrolysis of enzymatic/mild acidolysis lignin. Appl Energy 2011;88:316–22.

[9] Xu W, Miller SJ, Agrawal PK, Jones CW. Depolymerization and hydrodeoxygenation of switchgrass lignin with formic acid. ChemSusChem 2012;5:667–75.

[10] Saisu M, Sato T, Watanabe M, Adschiri T, Arai K. Conversion of lignin with supercritical water–phenol mixtures. Energy Fuels 2003;17:922–8.

[11] Yang Y, Gilbert A, Xu C. Hydrodeoxygenation of bio-crude in supercritical hexane with sulfided CoMo and CoMoP catalysts supported on MgO: a model compound study using phenol. Appl Catal A – Gen 2009;360:242–9.

[12] Bredenberg JBS, Huuska M, Räty J, Korpio M. Hydrogenolysis and hydrocracking of the carbon–oxygen bond: I. Hydrocracking of some simple aromatic O-compounds. J Catal 1982;77:242–7.

[13] Bunch AY, Wang X, Ozkan US. Hydrodeoxygenation of benzofuran over sulfided and reduced Ni–Mo/γ-Al_2O_3 catalysts: effect of H_2S. J Mol Catal A – Chem 2007;270:264–72.

[14] Xu Y, Wang T, Ma L, Zhang Q, Liang W. Upgrading of the liquid fuel from fast pyrolysis of biomass over MoNi/γ-Al_2O_3 catalysts. Appl Energy 2010;87:2886–91.

[15] Bui VN, Laurenti D, Afanasiev P, Geanter C. Hydrodeoxygenation of guaiacol with CoMo catalysts. Part I: Promoting effect of cobalt on HDO selectivity and activity.. Appl Catal B: Environ 2011;101:239–45.

[16] Bui VN, Laurenti D, Delichère P. Hydrodeoxygenation of guaiacol Part II: Support effect for CoMoS catalysts on HDO activity and selectivity. Appl Catal B: Environ 2011;101:246–55.

[17] Laurent M, Delmon B. Influence of water in the deactivation of a sulfided NiMo/γ-Al_2O_3 catalyst during hydrodeoxygenation. J Catal 1994;146:281–91.

[18] Zhang X, Wang T, Ma L, Wu C. Aqueous-phase catalytic process for production of pentane from furfural over nickel-based catalysts. Fuel 2010;89:2697–702.

[19] Chen WH, Ko HH, Sakthivel A, Huang SJ, Liu SH, Lo AY, et al. A solid-state NMR, FT-IR and TPD study on acid properties of sulfated and metal-promoted zirconia: influence of promoter and sulfation treatment. Catal Today 2006;116:111–20.

[20] Tarafdar A, Panda AB, Pramanik P. Synthesis of ZrO_2–SiO_2 mesocomposite with high ZrO_2 content via novel sol–gel method. Microporous Mesoporous Mater 2005;84:223–8.

[21] Rana MS, Srinivas BN, Maity SK, Dha GM, Prasada Rao TSR. Origin of cracking functionality of sulfided (Ni) CoMo/SiO_2–ZrO_2 catalysts. J Catal 2000;195:31–7.

[22] Gandarias I, Barrio VL, Requies J, Arias PL, Cambra JF, Güemez MB. From biomass to fuels: hydrotreating of oxygenated compounds. Int J Hydrogen Energy 2008;33:3485–8.

[23] Zhao C, Kou Y, Angeliki AL, Li X, Lercher JA. Highly selective catalytic conversion of phenolic bio-oil to alkanes. Angew Chem Int Ed 2009;48:3987–90.